Published in final edited form as:

Dev Biol. 2016 July 15; 415(2): 306–313. doi:10.1016/j.ydbio.2015.06.014.

Constitutively active mutation of ACVR1 in oral epithelium causes submucous cleft palate in mice

Kazuo Noda[a], **Yuji Mishina**[b], and **Yoshihiro Komatsu**[a,c]

[a]Department of Pediatrics, The University of Texas Medical School at Houston, Houston, TX, 77030, USA

[b]Department of Biologic and Materials Science, School of Dentistry, University of Michigan, Ann Arbor, MI, 48109, USA

[c]Graduate Program in Genes and Development, The University of Texas Graduate School of Biomedical Sciences at Houston, Houston, TX, 77030, USA

Abstract

Cleft palate is among the most common human birth defects. Submucous cleft palate (SMCP) is a subgroup of cleft palate, which may be as common as overt cleft palate. Despite the high frequency of SMCP in humans, only recently have several animal models of SMCP begun to provide insight into the mechanisms by which SMCP develops. In this study, we show that enhanced BMP signaling through constitutively active ACVR1 in palatal epithelium causes submucous cleft palate in mice. In these mutant mice, the fusion of both palatal mesenchyme in hard palate, and muscles in soft palate were hampered by epithelial tissue. During palatal fusion, enhanced SMAD-dependent BMP signaling impaired cell death and altered cell proliferation rate in medial edge epithelium (MEE), and resulted in MEE persistence. At the molecular level, downregulation of ΔNp63, which is crucial for normal palatal fusion, in MEE cells was impaired, leading to a reduction in caspase-3 activation. Our study provides a new insight into the etiology of SMCP caused by augmented BMP signaling.

Keywords

BMP; craniofacial development; ΔNp63; medial edge epithelium; palatogenesis

Introduction

Cleft palate, a split in the roof of the mouth, is among the most common human birth defects (Dixon et al., 2011). In mammals, the palate separates the oral cavity from the nasal cavity. It is comprised of an anterior bony hard palate and a posterior muscular soft palate. The soft

Corresponding author: Yoshihiro Komatsu, Department of Pediatrics, The University of Texas Medical School at Houston, 6431 Fannin St, Houston, TX, 77030, USA, Tel: +1-713-500-5783, Fax: +1-713-500-5689, Yoshihiro.Komatsu@uth.tmc.edu.

palate is movable and closes off the nasal airway during swallowing and speech. Submucous cleft palate (SMCP), the cleft of a posterior muscular palate with continuous lining of the roof of the mouth, is a subgroup of cleft palate, which may be as common as overt cleft palate (Garcia Velasco et al., 1988; Weatherley-White et al., 1972). Classic SMCP is identified by the triad of a bifid uvula, a furrow along the midline of the soft palate, and a notch in the posterior margin of the hard palate. The underlying anatomic abnormality consists of the improper insertion of the levator veli palatini muscles and other muscles in the soft palate onto the hard palate instead of forming muscle slings across the midline of the palate. In a condition designated as occult SMCP, the same muscle malposition is identified without overt signs of a bifid uvula and a furrow along the midline of the soft palate (Kaplan, 1975). Muscle malposition may be responsible for velopharyngeal insufficiency with hypernasal resonance during speech, feeding difficulties, and otitis media-related hearing loss (Stal and Hicks, 1998). Thus, both classic and occult types of SMCP are of clinical significance.

Several studies have identified the molecular and cellular mechanisms responsible for submucous cleft of the hard palate using genetically manipulated mouse models (Bush and Jiang, 2012). Loss of TGFβ signaling in the basal epithelium in mice results in medial edge epithelium (MEE) persistence and complete cleft of the soft palate (Dudas et al., 2006; Lane et al., 2015; Xu et al., 2006). Palatal mesenchyme-specific deletion of *Bmpr1a* impairs palatal shelf growth and bone development, and causes submucous cleft of the hard palate (Baek et al., 2011). Mice lacking *Tbx22* also showed reduced palatal bone formation at the posterior palatal region following complete fusion of mesenchymal tissue without MEE persistence (Pauws et al., 2009). Although MEE persistence is proposed as one of the mechanisms responsible for SMCP, little is known about the etiology of SMCP without cleft soft palate due to a lack of mutant mouse models mimicking classical or occult SMCP in humans.

The bone morphogenetic protein (BMP) signaling pathway plays a pivotal role in embryonic development, including craniofacial morphogenesis (Mishina and Snider, 2014; Nie et al., 2006). BMP signaling is propagated through BMP type I receptors (ALK1, ACVR1 or ALK2, BMPRIA or ALK3, and BMPRIB or ALK6) and type II receptors, both of which are transmembrane serine-threonine kinase receptors. Upon ligand binding, the BMP type II receptor associates with and phosphorylates the BMP type I receptor in the GS domain rich in glycine and serine. Then the BMP type I receptor phosphorylates the intracellular proteins SMAD1/5/8. Phosphorylated SMAD1/5/8 binds SMAD4 and translocates to the nucleus, where they complex with transcription factors and regulate target gene transcription (Mishina, 2003; Miyazono et al., 2010). In addition to this canonical (SMAD-dependent) pathway, the BMP receptor complex can also activate non-canonical (SMAD-independent) pathways, including mitogen-activated protein kinase (MAPK) signaling (Derynck and Zhang, 2003).

During palatal development, all BMP receptors, along with several BMPs and BMP antagonists, are expressed in dynamic and differential patterns along the anterior-posterior axis of palatal shelves. Among BMP receptors, the importance of the type I receptor BMPRIA in the development of palatal mesenchyme has been demonstrated by loss-of-

function studies in mice (Baek et al., 2011; Li et al., 2011; Liu et al., 2005). Although *Bmpr1a* is expressed in palatal epithelium (Li et al., 2013), the epithelial-specific inactivation of *Bmpr1a* shows no cleft palate phenotype (Andl et al., 2004). Moreover, explant culture of secondary palate from mice in which *Bmpr1a* was deleted in the epithelium of the maxillary process exhibits normal palatal fusion following MEE degradation, suggesting that BMPRIA expression in palatal epithelium is not required for palatal fusion (Liu et al., 2005). On the other hand, recent studies indicate that augmentation of BMP signaling causes cleft palate due to reduced cell proliferation in the anterior palatal mesenchyme (He et al., 2010; Li et al., 2013). Interestingly, *Noggin* knockout mice exhibit increased epithelial cell proliferation in the oral side palatal epithelium, where *Noggin* is normally expressed. This suggests that BMP signaling positively modulates cell proliferation in the palatal epithelium (He et al., 2010). In addition, increased BMP signaling in the oral epithelium of *Noggin*-deficient mice leads to ectopic periderm cell death in the posterior palate, and abnormal palate-mandibular adhesion. This has been also observed in mice with overexpression of the constitutively active form of BMPRIA in oral epithelium (He et al., 2010). In these mice, however, the effect of enhanced BMP signaling on the MEE cells is not addressed because palatal shelf elevation was prevented.

Here, we show that enhanced BMP signaling through constitutively active ACVR1 (caACVR1) in palatal epithelium causes SMCP in mice. In these mutant mice, the fusion of palatal mesenchyme in the hard palate and muscles in the soft palate was hampered by epithelial tissue. Previous paper demonstrated that using palatal explant culture, caACVR1 may have an impact on MEE during palatogenesis (Dudas et al., 2004a). However, it remains elusive if the augmentation of BMP signaling via ACVR1 dysregulates the fate of MEE in vivo. The purpose of this study is to clarify the effect of caACVR1 on MEE cell fate during palatal fusion in vivo. Our data demonstrate that enhanced SMAD-dependent BMP signaling impairs cell death and increases cell proliferation rates in MEE, and gives rise to MEE persistence presumably due to the upregulation of ΔNp63 and resulting reduction of caspase-3 activation in MEE.

Materials and Methods

Mice

To generate *caACVR1;K14-Cre* mice, we mated mice carrying the *caACVR1* allele (Fukuda et al., 2006) with mice carrying the *K14-Cre* allele (Dassule et al., 2000). The *K14-Cre* mice were obtained from the Jackson Laboratory. Genotyping was performed by PCR as previously described (Fukuda et al., 2006). Use of animals in this study was approved by the Animal Welfare Committee, the Institutional Animal Care and Use Committee of the University of Texas Health Science Center at Houston.

Histological analysis, immunohistochemistry, and immunofluorescence

Mouse embryos were fixed in 4% paraformaldehyde at 4°C overnight, and embedded in paraffin. Embryos were serially sectioned (7 μm thickness). Sections were kept on Superfrost Plus glass slides (Fisher Scientific). The paraffin sections were deparaffinized in xylene, and rehydrated in a descending series of ethanol solutions. Hematoxylin-eosin

staining was performed according to the standard protocol. For immunohistochemical and immunofluorescent staining, sections were subjected to antigen retrieval by the use of Antigen Unmasking Solution (Vector Laboratories, H-3300) for 20 min at 100°C. Then slides were washed in water, permeabilized with 0.1% TritonX-100 in PBS (PBST) or in TBS (TBST) for 15 min, and then blocked by incubation with 5% sheep serum in PBST or TBST for 30 min. The slides were incubated overnight at 4°C with antibodies against pSMAD1/5/8 (1:50, Cell Signaling, #9511), pp38 (1:500, Cell Signaling, #4511), pERK (1:500, Cell Signaling, #4376), pJNK (1:100, Cell Signaling, #4668), Ki67 (1:100, BD, 550609), ΔNp63 (1:500, BioLegend, Poly6190), cleaved caspase-3 (1:500, Cell signaling, #9664), pSMAD2 (1:100, Cell Signaling, #3101). For immunohistochemistry, after washing three times in PBST or TBST for 5 min, slides were incubated with biotinylated secondary antibodies followed by the addition of preformed ABC reagent (Santa Cruz, sc-2018). Immunoreactive cells were visualized using 3,3-diaminobenzidine substrate solution (Sigma-Aldrich, D4168) as a chromogen, and counterstained with hematoxylin. For immunofluorescence, after washing three times in PBST for 5 min, slides were incubated with Alexa Fluor 488-, Alexa Fluor 568- or Alexa Fluor 647-conjugated secondary antibodies (Life Technologies), followed by staining with Hoechst 33342 (Life Technologies). The slides were viewed with an Olympus FluoView FV1000 laser scanning confocal microscope by using the FV10-ASW Viewer (Ver. 3.1).

For frozen sections, mouse embryos were fixed in 4% paraformaldehyde at 4°C overnight, and embedded in Tissue-Plus O.C.T. Compound (Fisher Scientific). Embryos were serially sectioned (10 μm thickness). Sections were kept on Superfrost Plus glass slides (Fisher Scientific). Slides were washed and permeabilized with 0.1% TritonX-100 in PBST for 15 min, and then blocked by incubation with 5% sheep serum in PBST for 30 min. The slides were incubated overnight at 4°C with antibodies against HA (1:50, Cell Signaling, #3724), GFP (1:250, Life Technologies, A11122; 1:500, Abcam, ab13970), TGFβ3 (1:100, Santa Cruz, sc-82), IRF6 (1:100, Sigma-Aldrich, SAB2102995).

TUNEL assay

Paraffin sections (7 μm thickness) were treated with Trypsin-EDTA (0.25%) (Life Technologies) for 30 min at 37°C, and then subjected to TUNEL staining using the *In Situ* Cell Death Detection Kit, Fluorescein (Roche) following the manufacturer's protocol, and then counterstained with Hoechst 33342 (Life Technologies).

RNA in situ hybridization

Paraffin sections were hybridized as previously described (Komatsu et al., 2014). Antisense probes were used for detecting endogenous expression of *Acvr1* (Dudas et al., 2004b).

Statistical analysis

A Student's *t*-test was applied for statistical analysis. A *P*-value of less than 0.05 was considered statistically significant.

Results

Mice with epithelial *caACVR1* develop SMCP due to the persistence of medial edge epithelium (MEE)

To investigate the effect of enhanced BMP signaling mediated through constitutively active ACVR1 (caACVR1) on epithelial tissue, we crossed the mice carrying the *caACVR1* transgene (Fukuda et al., 2006) with the mice expressing the *Keratin (K)-14* promoter driven *Cre* recombinase (Dassule et al., 2000). The resulting mutant (hereafter *caACVR1;K14-Cre*) newborn mice died within 24 hours of birth, and lacked milk in their stomachs (Fig. 1A). Macroscopic examination showed that the primary palate failed to fuse with secondary palate (Fig. 1B–D), and a white strip was found in the midline of the secondary palate including soft palate in *caACVR1;K14-Cre* mice (Fig. 1B, C, E). Cleft soft palate was not observed in *caACVR1;K14-Cre* mice. These phenotypes were identified in *caACVR1;K14-Cre* newborn mice with 100% penetrance (n = 16).

Histological analysis confirmed that the anterior part of secondary palate failed to fuse in *caACVR1;K14-Cre* mice at E18.5 (Fig. 2A, B). In the middle of the secondary palate in *caACVR1;K14-Cre* embryos, the fusion of mesenchymal tissue was impaired by epithelial seam (Fig. 2C, D). In addition, an epithelial cyst-like tissue was identified intermittently at the midline of hard palate and soft palate (Fig. 2F, J, arrow). These epithelial tissues impaired mesenchymal fusion of the hard palate and muscle fusion of the soft palate (Fig. 2F, J, arrow head), suggesting that *caACVR1;K14-Cre* mice have SMCP without cleft soft palate. Previous studies have demonstrated that one of the causes of SMCP in mice is MEE persistence (Dudas et al., 2006; Lane et al., 2014; Xu et al., 2006). To elucidate whether SMCP found in *caACVR1;K14-Cre* mice is due to the MEE persistence, we focused on MEE seam formation at E14.5 and E15.5. Before E14.5, palatal elevation and palatal epithelial attachment occurred normally in *caACVR1;K14-Cre* embryos (data not shown). At E14.5, the MEE seam was formed in the palate of both control and mutant embryos (Fig. 2K, L). At E15.5, MEE was not present in the palate of control embryos (Fig. 2M), while the MEE seam was not degraded in the palate of *caACVR1;K14-Cre* mutants at E15.5 (Fig. 2N). These data demonstrate that the SMCP phenotype in *caACVR1;K14-Cre* mice is due to abnormal MEE persistence after proper MEE seam formation.

SMAD-dependent BMP signaling was activated in *caACVR1;K14-Cre* MEE cells

First, we analyzed the expression levels of endogenous *Acvr1* and ectopic caACVR1 before and during palatal fusion. In situ hybridization revealed that endogenous *Acvr1* was expressed in palatal epithelia as well as in mesenchyme at E13.5 and E14.5 (Supplementary Fig. S1A, B). To identify the expression of ectopic caACVR1, we performed immunostaining for HA and EGFP. After Cre-mediated recombination of the transgene, EGFP is expressed along with HA-tagged caACVR1 (Fukuda et al., 2006). HA and EGFP was detected in the palatal epithelium at E13.5 and in MEE at E14.5 (Supplementary Fig. S1C–J). These data suggest that caACVR1 was expressed in *caACVR1;K14-Cre* MEE during palatal fusion.

Since BMP signaling activates both SMAD-dependent and SMAD-independent signaling pathways (Derynck and Zhang, 2003), we investigated which pathways are responsible for the MEE persistence in *caACVR1;K14-Cre* embryos. Immunohistochemical analysis showed that phosphorylated SMAD1/5/8 (pSMAD1/5/8) levels were significantly increased in *caACVR1; K14-Cre* MEE cells compared to those in control MEE cells at E14.5 (Fig. 3A, B). On the other hand, levels of SMAD-independent BMP signaling mediators, phosphorylated p38 (pp38), phosphorylated ERK (pERK), and phosphorylated JNK (pJNK), were comparable in both control and *caACVR1;K14-Cre* MEE cells (Fig. 3C–H). These data suggest that the MEE persistence in *caACVR1;K14-Cre* mice is possibly due to the activation of SMAD-dependent BMP signaling through caACVR1.

Enhanced BMP signaling via caACVR1 affects the fate of MEE

Since apoptosis is one of the mechanisms of the MEE disintegration during palatal fusion (Cuervo and Covarrubias, 2004), we first examined the apoptotic activities in both control and *caACVR1;K14-Cre* MEE with a TUNEL assay. A considerable number of apoptotic cells were found in control MEE at E14.5 (Fig. 4A), while a significant reduction of apoptotic cells was observed in *caACVR1;K14-Cre* MEE (Fig. 4B, E). At E15.5, the remaining MEE in control mice underwent apoptosis (Fig. 4C), whereas apoptotic activity of persistent MEE in mutant embryos was still low (Fig. 4D). Next, we analyzed cell proliferation in MEE at E14.5 and E15.5. Staining of Ki67 at E14.5 revealed that Ki67-positive cells are slightly but significantly increased in *caACVR1;K14-Cre* MEE, compared to control MEE (Fig. 4F, G, J). Examination of Ki67 expression at E15.5 revealed that control MEE cells did not have proliferation ability, while mutant MEE cells still maintain the ability to proliferate (Fig. 4H, I). These data suggest that enhanced BMP signaling via caACVR1 prevents MEE apoptosis and increases cell proliferation ability of MEE cells.

Upregulation of ΔNp63 is responsible for MEE persistence in *caACVR1;K14-Cre* mice

Recent studies have revealed that downregulation of ΔNp63 in MEE occurs during normal palatal fusion (Fakhouri et al., 2012; Hu et al., 2014; Thomason et al., 2010), and increased expression of ΔNp63 in MEE is detected in *Tgfbr2*$^{fl/fl}$*;K14-Cre* embryos in which MEE persistence occurs (Iwata et al., 2013). In addition, the expression of ΔNp63 is known to be regulated by BMP signaling (Bakkers et al., 2002; Medawar et al., 2008; Tribulo et al., 2012). Therefore, we hypothesized that augmentation of BMP signaling upregulates the expression of ΔNp63 in *caACVR1;K14-Cre* MEE cells. Immunofluorescent staining showed that the ΔNp63 staining in *caACVR1;K14-Cre* MEE was relatively high compared to that in control MEE at E14.5 (Fig. 5A, B). To examine further if enhanced BMP signaling via caACVR1 have an influence on TGFβ signaling and IRF6 expression, which are critical during palatogenesis (Dudas et al., 2006; Iwata et al., 2013), we examined expressions of TGFβ3, phosphorylated SMAD2 (pSMAD2), and IRF6 in MEE. The results showed that the expression levels of TGFβ3, pSMAD2, and IRF6 were comparable between control and *caACVR1;K14-Cre* MEE cells (Supplementary Fig. S2A–F), suggesting enhanced BMP signaling through caACVR1 in MEE does not affect TGF-β signaling during palatogenesis.

To address whether ΔNp63 expression is regulated by caACVR1 cell-autonomously or non-cell-autonomously, we performed co-staining of EGFP and ΔNp63. The results

demonstrated that most of the cells expressing ΔNp63 in *caACVR1;K14-Cre* MEE seam were positive for EGFP (Fig. 5C, D), suggesting that ΔNp63 expression in *caACVR1;K14-Cre* embryos was maintained by enhanced BMP signaling through caACVR1 in cell-autonomous manner.

Since it has been reported that increased ΔNp63 expression by BMP signaling downregulates the transcription of apoptotic factors (Tribulo et al., 2012), we postulated that ΔNp63 is the mediator between enhanced BMP signaling and reduction of cell death through inhibiting the expression of apoptotic factors such as caspase-3 during MEE disintegration. Indeed, activated caspase-3 expression was decreased in *caACVR1;K14-Cre* MEE (Fig. 5E, F), suggesting that enhanced SMAD-dependent BMP signaling sustains the expression of ΔNp63, thus preventing caspase-dependent cell death in MEE during palatal fusion (Fig. 5G).

Discussion

In this study, we investigated the effect of aberrant BMP signaling on oral epithelium using *caACVR1* transgenic mice with a *K14-Cre* driver, in which SMAD1/5/8 are constitutively phosphorylated in ectodermal tissues. Our results indicate that enhanced BMP signaling through caACVR1 in the oral epithelium causes SMCP due to MEE persistence. It has been reported that Noggin-deficient mice show complete cleft palate which is also observed in mice with constitutively active mutation of BMPR1A driven by K14-Cre (*caBMPR1A;K14-Cre*) (He et al., 2010). While *Noggin* mutants show an ectopic apoptosis in palatal epithelium, augmentation of BMP signaling through ACVR1 resulted in downregulation of cell death accompanied with upregulation of ΔNp63 in MEE at E14.5. This suggests that caACVR1 may impact palatal epithelium differently from *Noggin* mutants or *caBMPR1A;K14-Cre* mice. However, we cannot exclude the possibility that insufficient Cre-mediated recombination in *caACVR1;K14-Cre* mice may be attributed to a complete different phenotype. Although we confirmed the expression of caACVR1 and EGFP in the palatal epithelium at E13.5 and E14.5 (Supplementary Fig. S1C–J), the HA- or EGFP-positive cells were limited, suggesting the number of cell population with enhanced BMP signaling in *caACVR1;K14-Cre* embryos is relatively small compared with *Noggin* mutants or *caBMPR1A;K14-Cre* mice.

We found that apoptosis of the MEE cells in *caACVR1;K14-Cre* embryos at E14.5 was significantly decreased compared to that in control embryos. This is an interesting result, because BMPs are generally recognized as potent inducers of cell death during embryonic development (Graham et al., 1994; Hayano et al., 2015; Macias et al., 1997). However, Cuervo et al. found that endogenous BMP signaling is not required for cell death in MEE, and that exogenous BMPs were not able to induce cell death in palatal tissue in a palatal explant culture system (Cuervo et al., 2002). In agreement with these results, our *in vivo* study shows that aberrant BMP signaling causes a decrease in cell death in MEE during palatal fusion.

In *caACVR1;K14-Cre* mutant embryos, downregulation of ΔNp63 in MEE cells was decreased during palatal fusion. Since ΔNp63 expression is induced by BMP signaling in

murine ES cells during epidermal differentiation (Medawar et al., 2008), and in ectoderm of zebrafish (Bakkers et al., 2002) and *Xenopus* (Tribulo et al., 2012), it is possible that ΔNp63 upregulation in *caACVR1;K14-Cre* MEE is caused by enhanced BMP-SMAD signaling. We also identified a reduction of cleaved caspase-3 protein levels in *caACVR1;K14-Cre* MEE. It has been suggested that ΔNp63 acts as an anti-apoptotic factor (Carroll et al., 2006; Cheng et al., 2006; Tribulo et al., 2012), therefore upregulation of ΔNp63 by augmented BMP signaling may suppress caspase-dependent cell death in *caACVR1;K14-Cre* MEE during palatal fusion.

While there are several mouse models that mimic human SMCP, these mutants show severe cleft palate: cleft soft palate in $Tgfbr2^{fl/fl}$;*K14-Cre* (Xu et al., 2006), palatal bone defects in $Bmpr1a^{fl/fl}$;*Osr2-Cre* mice (Baek et al., 2011) and *Tbx22* knockout mice (Pauws et al., 2009), in addition to mesenchymal fusion defects. The c*aACVR1;K14-Cre* mice show neither an overt cleft of soft palate nor a defect in palatal bone development; however, the fusion of the muscles in the soft palate is in part prevented by the abnormal persistence of the MEE seam. Thus, *caACVR1;K14-Cre* mice may serve as a unique animal model that recapitulates the occult type of SMCP in humans. Further analysis of these mice may provide better understanding of the etiology of cleft palate in human.

Supplementary Material

Refer to Web version on PubMed Central for supplementary material.

Acknowledgments

We thank Dr. Vesa Kaartinen for providing us in situ plasmids; Dr. Bridget DeLay for critical reading of this manuscript and Dr. Junichi Iwata for fruitful discussion. This work was supported by the grant from the NIDCR/NIH R00DE021054 to YK, R01DE020843 to YM, and by a fellowship from The Uehara Memorial Foundation to KN.

References

Andl T, Ahn K, Kairo A, Chu EY, Wine-Lee L, Reddy ST, Croft NJ, Cebra-Thomas JA, Metzger D, Chambon P, Lyons KM, Mishina Y, Seykora JT, Crenshaw EB 3rd, Millar SE. Epithelial Bmpr1a regulates differentiation and proliferation in postnatal hair follicles and is essential for tooth development. Development (Cambridge, England). 2004; 131:2257–2268.

Baek JA, Lan Y, Liu H, Maltby KM, Mishina Y, Jiang R. Bmpr1a signaling plays critical roles in palatal shelf growth and palatal bone formation. Developmental biology. 2011; 350:520–531. [PubMed: 21185278]

Bakkers J, Hild M, Kramer C, Furutani-Seiki M, Hammerschmidt M. Zebrafish DeltaNp63 is a direct target of Bmp signaling and encodes a transcriptional repressor blocking neural specification in the ventral ectoderm. Developmental cell. 2002; 2:617–627. [PubMed: 12015969]

Bush JO, Jiang R. Palatogenesis: morphogenetic and molecular mechanisms of secondary palate development. Development (Cambridge, England). 2012; 139:231–243.

Carroll DK, Carroll JS, Leong CO, Cheng F, Brown M, Mills AA, Brugge JS, Ellisen LW. p63 regulates an adhesion programme and cell survival in epithelial cells. Nature cell biology. 2006; 8:551–561. [PubMed: 16715076]

Cheng W, Jacobs WB, Zhang JJ, Moro A, Park JH, Kushida M, Qiu W, Mills AA, Kim PC. DeltaNp63 plays an anti-apoptotic role in ventral bladder development. Development (Cambridge, England). 2006; 133:4783–4792.

Cuervo R, Covarrubias L. Death is the major fate of medial edge epithelial cells and the cause of basal lamina degradation during palatogenesis. Development (Cambridge, England). 2004; 131:15–24.

Cuervo R, Valencia C, Chandraratna RA, Covarrubias L. Programmed cell death is required for palate shelf fusion and is regulated by retinoic acid. Developmental biology. 2002; 245:145–156. [PubMed: 11969262]

Dassule HR, Lewis P, Bei M, Maas R, McMahon AP. Sonic hedgehog regulates growth and morphogenesis of the tooth. Development (Cambridge, England). 2000; 127:4775–4785.

Derynck R, Zhang YE. Smad-dependent and Smad-independent pathways in TGF-beta family signalling. Nature. 2003; 425:577–584. [PubMed: 14534577]

Dixon MJ, Marazita ML, Beaty TH, Murray JC. Cleft lip and palate: understanding genetic and environmental influences. Nature reviews Genetics. 2011; 12:167–178.

Dudas M, Kim J, Li WY, Nagy A, Larsson J, Karlsson S, Chai Y, Kaartinen V. Epithelial and ectomesenchymal role of the type I TGF-beta receptor ALK5 during facial morphogenesis and palatal fusion. Developmental biology. 2006; 296:298–314. [PubMed: 16806156]

Dudas M, Nagy A, Laping NJ, Moustakas A, Kaartinen V. Tgf-beta3-induced palatal fusion is mediated by Alk-5/Smad pathway. Developmental biology. 2004a; 266:96–108. [PubMed: 14729481]

Dudas M, Sridurongrit S, Nagy A, Okazaki K, Kaartinen V. Craniofacial defects in mice lacking BMP type I receptor Alk2 in neural crest cells. Mechanisms of development. 2004b; 121:173–182. [PubMed: 15037318]

Fakhouri WD, Rhea L, Du T, Sweezer E, Morrison H, Fitzpatrick D, Yang B, Dunnwald M, Schutte BC. MCS9.7 enhancer activity is highly, but not completely, associated with expression of Irf6 and p63. Developmental dynamics: an official publication of the American Association of Anatomists. 2012; 241:340–349. [PubMed: 22113860]

Fukuda T, Scott G, Komatsu Y, Araya R, Kawano M, Ray MK, Yamada M, Mishina Y. Generation of a mouse with conditionally activated signaling through the BMP receptor, ALK2. Genesis (New York, NY: 2000). 2006; 44:159–167.

Garcia Velasco M, Ysunza A, Hernandez X, Marquez C. Diagnosis and treatment of submucous cleft palate: a review of 108 cases. The Cleft palate journal. 1988; 25:171–173. [PubMed: 3259168]

Graham A, Francis-West P, Brickell P, Lumsden A. The signalling molecule BMP4 mediates apoptosis in the rhombencephalic neural crest. Nature. 1994; 372:684–686. [PubMed: 7990961]

Hayano S, Komatsu Y, Pan H, Mishina Y. Augmented BMP signaling in the neural crest inhibits nasal cartilage morphogenesis by inducing p53-mediated apoptosis. Development (Cambridge, England). 2015; 142:1357–1367.

He F, Xiong W, Wang Y, Matsui M, Yu X, Chai Y, Klingensmith J, Chen Y. Modulation of BMP signaling by Noggin is required for the maintenance of palatal epithelial integrity during palatogenesis. Developmental biology. 2010; 347:109–121. [PubMed: 20727875]

Hu L, Liu J, Li Z, Ozturk F, Gurumurthy C, Romano RA, Sinha S, Nawshad A. TGFbeta3 Regulates Periderm Removal through DeltaNp63 in the Developing Palate. Journal of cellular physiology. 2014

Iwata J, Suzuki A, Pelikan RC, Ho TV, Sanchez-Lara PA, Urata M, Dixon MJ, Chai Y. Smad4-Irf6 genetic interaction and TGFbeta-mediated IRF6 signaling cascade are crucial for palatal fusion in mice. Development (Cambridge, England). 2013; 140:1220–1230.

Kaplan EN. The occult submucous cleft palate. The Cleft palate journal. 1975; 12:356–368. [PubMed: 1058746]

Komatsu Y, Kishigami S, Mishina Y. In situ hybridization methods for mouse whole mounts and tissue sections with and without additional beta-galactosidase staining. Methods in molecular biology (Clifton, NJ). 2014; 1092:1–15.

Lane J, Yumoto K, Azhar M, Ninomiya-Tsuji J, Inagaki M, Hu Y, Deng C, Kim J, Mishina Y, Kaartinen V. Tak1, Smad4 and Trim33 redundantly mediate TGF-beta3 signaling during palate development. Developmental biology. 2014

Lane J, Yumoto K, Azhar M, Ninomiya-Tsuji J, Inagaki M, Hu Y, Deng CX, Kim J, Mishina Y, Kaartinen V. Tak1, Smad4 and Trim33 redundantly mediate TGF-beta3 signaling during palate development. Developmental biology. 2015; 398:231–241. [PubMed: 25523394]

Li L, Lin M, Wang Y, Cserjesi P, Chen Z, Chen Y. BmprIa is required in mesenchymal tissue and has limited redundant function with BmprIb in tooth and palate development. Developmental biology. 2011; 349:451–461. [PubMed: 21034733]

Li L, Wang Y, Lin M, Yuan G, Yang G, Zheng Y, Chen Y. Augmented BMPRIA-mediated BMP signaling in cranial neural crest lineage leads to cleft palate formation and delayed tooth differentiation. PloS one. 2013; 8:e66107. [PubMed: 23776616]

Liu W, Sun X, Braut A, Mishina Y, Behringer RR, Mina M, Martin JF. Distinct functions for Bmp signaling in lip and palate fusion in mice. Development (Cambridge, England). 2005; 132:1453–1461.

Macias D, Ganan Y, Sampath TK, Piedra ME, Ros MA, Hurle JM. Role of BMP-2 and OP-1 (BMP-7) in programmed cell death and skeletogenesis during chick limb development. Development (Cambridge, England). 1997; 124:1109–1117.

Medawar A, Virolle T, Rostagno P, de la Forest-Divonne S, Gambaro K, Rouleau M, Aberdam D. DeltaNp63 is essential for epidermal commitment of embryonic stem cells. PloS one. 2008; 3:e3441. [PubMed: 18927616]

Mishina Y. Function of bone morphogenetic protein signaling during mouse development. Frontiers in bioscience: a journal and virtual library. 2003; 8:d855–869. [PubMed: 12700086]

Mishina Y, Snider TN. Neural crest cell signaling pathways critical to cranial bone development and pathology. Experimental cell research. 2014; 325:138–147. [PubMed: 24509233]

Miyazono K, Kamiya Y, Morikawa M. Bone morphogenetic protein receptors and signal transduction. Journal of biochemistry. 2010; 147:35–51. [PubMed: 19762341]

Nie X, Luukko K, Kettunen P. BMP signalling in craniofacial development. The International journal of developmental biology. 2006; 50:511–521. [PubMed: 16741866]

Pauws E, Hoshino A, Bentley L, Prajapati S, Keller C, Hammond P, Martinez-Barbera JP, Moore GE, Stanier P. Tbx22null mice have a submucous cleft palate due to reduced palatal bone formation and also display ankyloglossia and choanal atresia phenotypes. Human molecular genetics. 2009; 18:4171–4179. [PubMed: 19648291]

Stal S, Hicks MJ. Classic and occult submucous cleft palates: a histopathologic analysis. The Cleft palate-craniofacial journal: official publication of the American Cleft Palate-Craniofacial Association. 1998; 35:351–358. [PubMed: 9684774]

Thomason HA, Zhou H, Kouwenhoven EN, Dotto GP, Restivo G, Nguyen BC, Little H, Dixon MJ, van Bokhoven H, Dixon J. Cooperation between the transcription factors p63 and IRF6 is essential to prevent cleft palate in mice. The Journal of clinical investigation. 2010; 120:1561–1569. [PubMed: 20424327]

Tribulo C, Guadalupe Barrionuevo M, Aguero TH, Sanchez SS, Calcaterra NB, Aybar MJ. DeltaNp63 is regulated by BMP4 signaling and is required for early epidermal development in Xenopus. Developmental dynamics: an official publication of the American Association of Anatomists. 2012; 241:257–269. [PubMed: 22170861]

Weatherley-White RC, Sakura CY Jr, Brenner LD, Stewart JM, Ott JE. Submucous cleft palate. Its incidence, natural history, and indications for treatment. Plastic and reconstructive surgery. 1972; 49:297–304. [PubMed: 5060321]

Xu X, Han J, Ito Y, Bringas P Jr, Urata MM, Chai Y. Cell autonomous requirement for Tgfbr2 in the disappearance of medial edge epithelium during palatal fusion. Developmental biology. 2006; 297:238–248. [PubMed: 16780827]

Highlights

- Enhanced BMP signaling through ACVR1 in epithelium causes palatal fusion defects
- Aberrant BMP-SMAD signaling alters the fate of medial edge epithelium (MEE)
- Enhanced BMP signaling upregulates Np63 resulting in reduction of caspase-3 in MEE

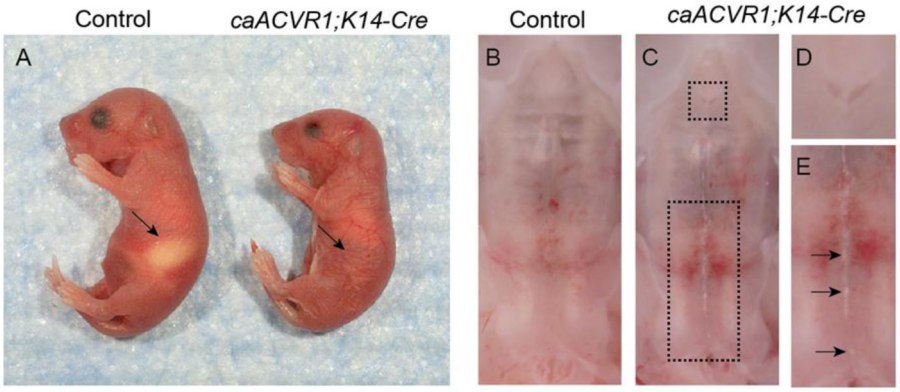

Fig. 1. Palatal defects are present in mice carrying epidermal-specific expression of *caACVR1*

(A) Control (left) and *caACVR1;K14-Cre* (right) newborns. Note the absence of milk in the stomach of the *caACVR1;K14-Cre* pups (arrow). (B) Normal palate development in control mouse. (C) Palate defects in *caACVR1;K14-Cre* mouse were shown enlarged in panels (D) and (E). The primary palate failed to fuse with secondary palate (D), and a white strip was observed in the midline of the secondary palate including soft palate (E, arrows). Note that cleft soft palate was not identified in *caACVR1;K14-Cre* mice.

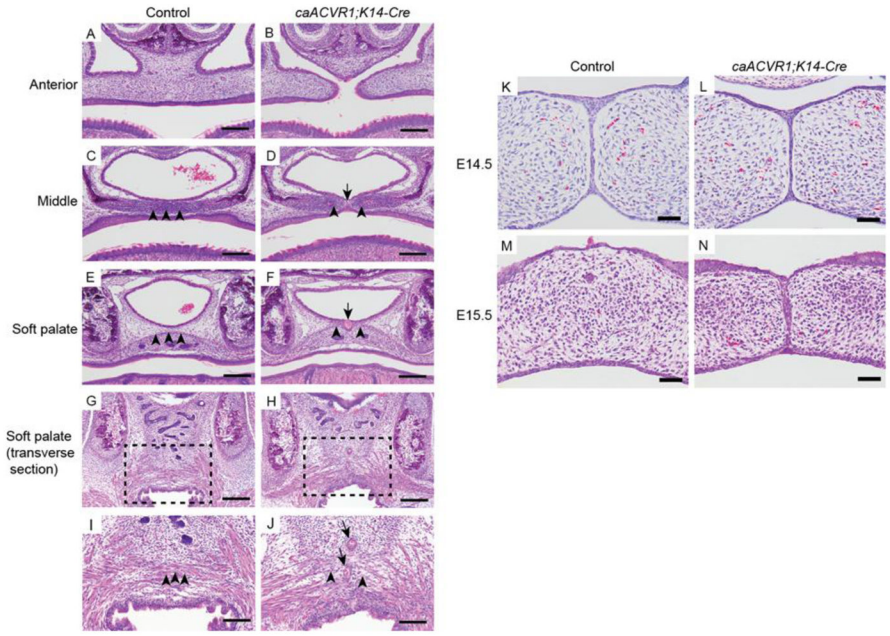

Fig. 2. Histological analysis of the palate of *caACVR1;K14-Cre* mutants

(A–N) H&E staining of control (A, C, E, G, I, K, M) and *caACVR1;K14-Cre* (B, D, F, H, J, L, N) palates at E18.5 (A–J), at E14.5 (K, L), and at E15.5 (M, N). (A, B) In control embryos, no fusion defect was found in the anterior secondary palate and nasal septum, while in *caACVR1;K14-Cre* embryos, palatal shelves of the anterior secondary palate failed to fuse with each other and with the nasal septum. (C, D) In the middle part of hard palate of control embryos, the fusion of palatal mesenchyme (arrowheads) was complete, while in *caACVR1;K14-Cre* embryo palates, the fusion of mesenchymal tissue (arrowheads) was impaired by the presence of an epithelial seam (arrow). (E, F) In the soft palate of control embryos, the tensor veli palatini muscle was fused (arrowheads), while in the soft palate of *caACVR1;K14-Cre* embryos, an epithelial cyst-like tissue (arrow) prevented the fusion of the tensor veli palatini muscle (arrowheads). (G–J) Transverse sections of the soft palates of control (G, I) and *caACVR1;K14-Cre* (H, J) embryos. Boxed areas in G and H are enlarged in I and J, respectively. Muscle fibers are fused in the soft palate of control embryos (arrowheads), while epithelial tissue (arrows) impaired the fusion of the muscle fibers in the soft palate of *caACVR1;K14-Cre* embryos (arrowheads). (K, L) MEE seams were identified both in control (K) and *caACVR1;K14-Cre* (L) palates at E14.5. (M, N) MEE seams persisted only in *caACVR1;K14-Cre* (N) palates at E15.5. Scale bars, 200 μm (A–H); 100 μm (I, J); 50 μm (K–N).

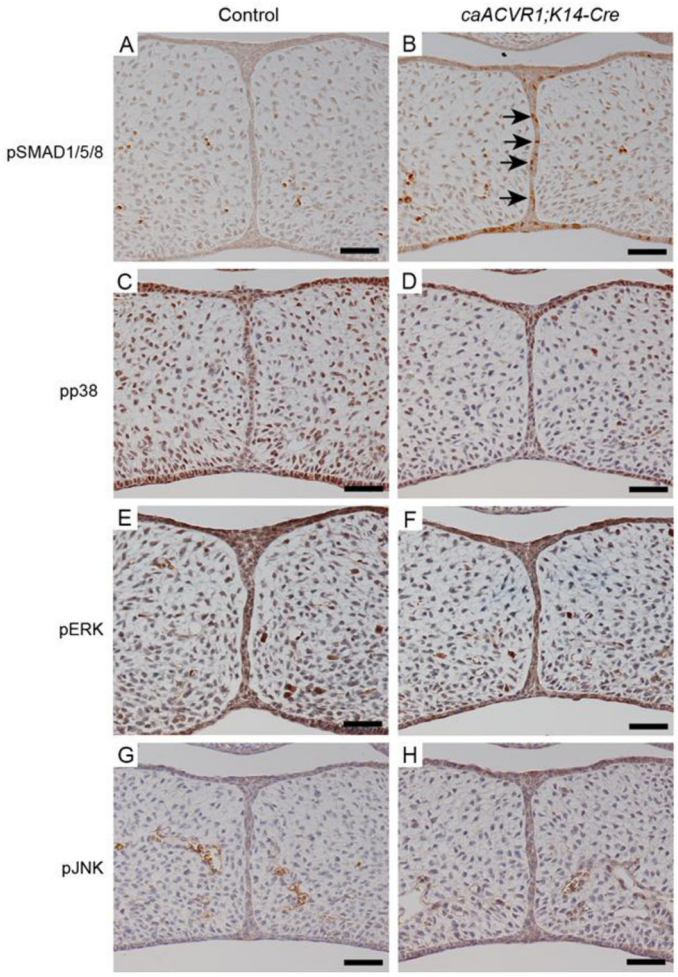

Fig. 3. BMP-SMAD signaling pathway was activated in *caACVR1;K14-Cre* MEE

(A–H) Immunohistochemical analysis of pSMAD1/5/8 (A, B), pp38 (C, D), pERK (E, F), and pJNK (G, H) of control (A, C, E, G) and *caACVR1;K14-Cre* (B, D, F, H) palates at E14.5. Brown, positive signal. Nuclei were counterstained with hematoxylin. Arrows in B indicate pSMAD1/5/8-positive MEE cells in a *caACVR1;K14-Cre* embryo. Scale bars, 50 μm.

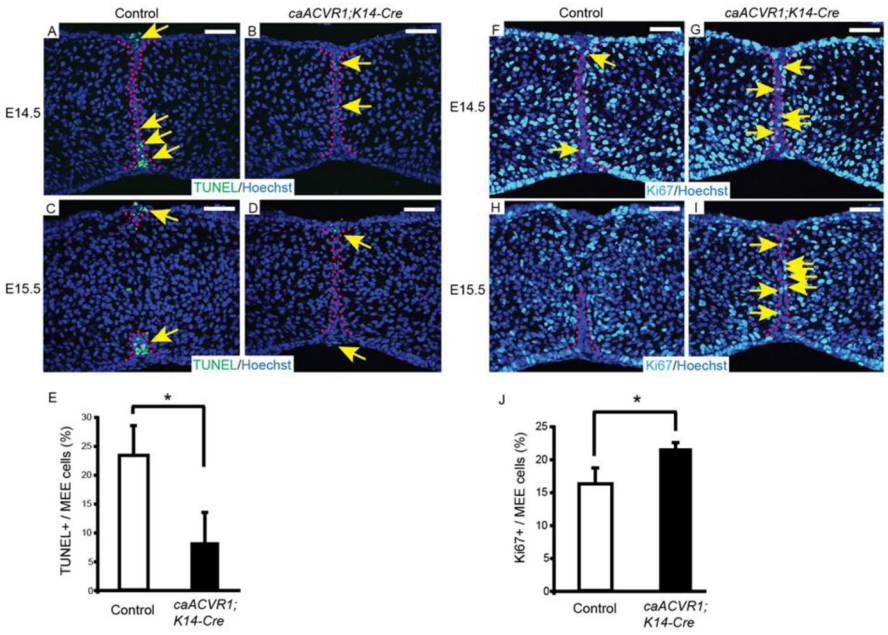

Fig. 4. The fate of MEE cells was altered in *caACVR1;K14-Cre* embryos

(A–D) TUNEL staining of sections of control (A, C) and *caACVR1;K14-Cre* (B, D) palates at E14.5 (A, B) and E15.5 (C, D). Red dashed lines outline the MEE cells. Arrows indicate TUNEL-positive cells (green) in the MEE. (E) Quantification of the number of TUNEL-positive cells in the MEE of control (n = 3) and *caACVR1;K14-Cre* (n = 3) palates at E14.5. Error bars represent s.d., **P* = 0.023. (F–I) Ki67 staining of sections of control (F, H) and *caACVR1;K14-Cre* (G, I) palates at E14.5 (F, G) and E15.5 (H, I). Red dashed lines outline the MEE cells. Arrows indicate Ki67-positive cells (light blue) in the MEE. (J) Quantification of the number of Ki67-positive cells in the MEE of control (n = 3) and *caACVR1;K14-Cre* (n = 3) palates at E14.5. Error bars represent s.d., **P* = 0.021. Scale bars, 50 μm.

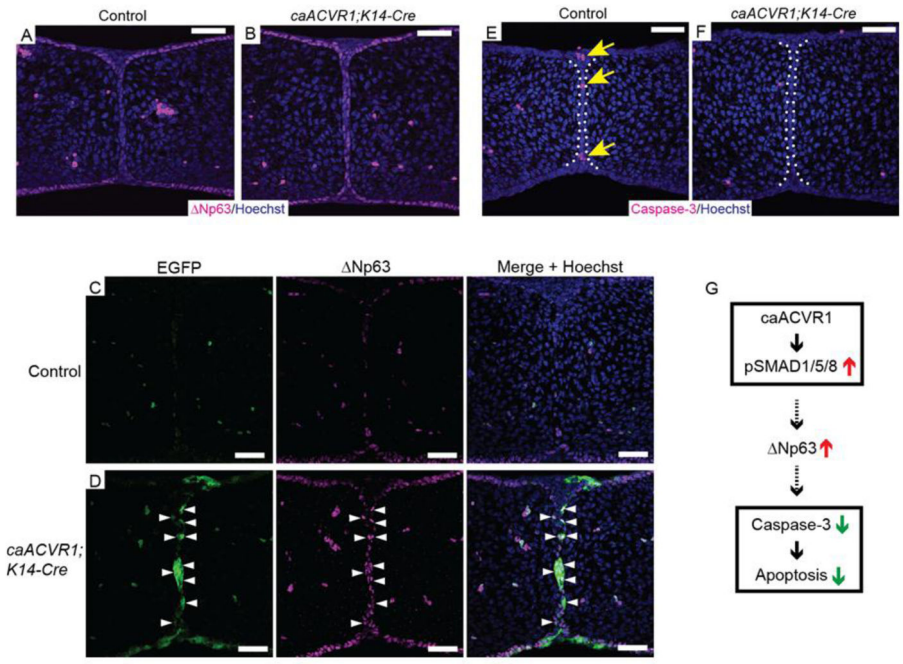

Fig. 5. Increased ΔNp63 expression in *caACVR1;K14-Cre* MEE cells

(A, B) Immunofluorescent staining for ΔNp63 in control (A) and *caACVR1;K14-Cre* (B) palates at E14.5. In control embryos, MEE cells have low expression of ΔNp63 (A), while MEE cells maintain high expression of ΔNp63 in *caACVR1;K14-Cre* embryos (B). (C, D) Immunofluorescent staining for EGFP and ΔNp63 in control (C) and c*aACVR1;K14-Cre* (D) palates at E14.5. Most of the MEE cells expressing ΔNp63 were positive for EGFP (D, arrowhead). (E, F) Cleaved caspase-3 staining of sections of control (E) and *caACVR1;K14-Cre* (F) palates at E14.5. Cleaved caspase-3 was detected in control MEE (E, arrows), while the expression level of cleaved caspase-3 was significantly reduced in *caACVR1;K14-Cre* MEE (F). (G) Schematic drawing representing the results of this study. Enhancement of SMAD-dependent BMP signaling via caACVR1 in MEE upregulates ΔNp63 expression and prevents caspase-dependent cell death during MEE disintegration. Scale bars, 50 μm.